Low-Complexity Integrated Optical-Electrical Quasi-Coherent RX Front End Supporting 5 km SSMF Transmission in C-band for 50G PON

Cheng Wang, Cédric Bruynsteen, Jakob Declercq, Joris Lambrecht, Bart Moeneclaey, Nishant Singh and Xin Yin

***Abstract*—An integrated balanced quasi-coherent receiver front end for 50G Passive Optical Network (PON) was designed and experimentally demonstrated. The received intensity modulated optical signal is boosted by a local oscillator (LO) laser and downconverted to an electrical intermediate frequency (IF) signal after integrated 2x2 multi-mode interference (MMI) and high-speed germanium photodiode (PD). By adjusting the wavelength offset between LO and transmitter laser, the IF can be chosen near the 3 dB bandwidth of RX front end to suppress the chromatic dispersion (CD) induced distortion in the upper sideband. After amplification by an integrated transimpedance amplifier (TIA), the baseband signal is demodulated via a simple square and low-pass-filter (LPF) function using offline digital signal processing (DSP). In contrast to traditional coherent receivers, no phase locking or carrier phase recovery is required. For 50 Gb/s non-return to zero(NRZ), corresponding to pre-FEC limit at bit error rate (BER) reference level 1e-2 in ITU-T G.9804, the measured optical modulated amplitude (OMA) sensitivity is -25.8 dBm (average received optical power is -27 dBm) in back-to-back (B2B) case and -19.8 dBm after 5 km standard single-mode-fiber (SSMF) transmission in C-band at 1550nm, without any CD compensation and equalization in DSP. Measurement results show that total chromatic dispersion of 85ps/nm can be handled for BER value lower than 1e-2. Compared with direct detection by using the same integrated high-speed germanium photodiode and TIA, the measured OMA sensitivity at BER reference level 1e-2 of the proposed quasi-coherent receiver has 13 dB improvement in B2B case and higher than 16 dB enhancement after 5 km SSMF transmission in C-band for 50 Gb/s NRZ with 10.1 dBm LO power. By reducing LO power for high-power input signals, >24 dB dynamic range is covered at BER reference level 1e-2, which satisfies class C+ level in ITU-T 50G PON PMD layer specification, assuming 8.5 dBm transmitter launch power.**

***Index Terms*—Quasi-Coherent, 50G PON, LO, OMA, BER, Chromatic Dispersion.**

I. Introduction

With the emergence of video/audio streaming, cloud computing, and the development of 5G networks with front, mid, and backhaul capabilities, there has been an exponential increase in demand for higher data rates across access networks. New Passive Optical Network (PON) standards with data rates exceeding 25 Gb/s have been proposed to satisfy these requirements, such as 50G PON PMD [1]. In upcoming 50G PON systems, the receiver in both ONU and OLT need to support 50 Gb/s detection. To satisfy such high data rate as well as fiber reach and optical budget, avalanche photodiodes (APDs) have been used in Intensity Modulation Direct Detection (IMDD) schemes [2] to enhance sensitivity thanks to their increased responsivity compared to PIN photodiodes. However, the avalanche multiplication process in APDs requires more time than photon to electron-hole pair conversion in high speed PIN PDs. The bandwidth (BW) of high gain APD is limited by finite gain-bandwidth product [3], which further limits the BW of receiver front end. Thus, complex equalization is needed in Digital Signal Processing (DSP) for data rates beyond 25 Gb/s [2]. In [4] and [5], a semiconductor optical amplifier (SOA) provides optical pre-amplification and the use of a PIN photodiode is maintained. Though [5] achieves good sensitivity in B2B case at 50 Gb/s NRZ without complex equalization, chromatic dispersion after long-distance transmission in Standard Single-Mode Fibre (SSMF) results in severe signal degradation, which needs to be compensated by complex DSP. In addition to the cost increase from using either an APD or SOA, dispersion-compensation DSP increases both the cost and power consumption. Though moving from C-band to O-band can partially alleviate the problem, thanks to lower chromatic dispersion in O-band, equalization for compensating chromatic dispersion is usually required as the data rate goes beyond 25 Gb/s. Coherent detection is regarded as a potential candidate for satisfying the requirements set by high-rate optical access networks [6]. However, higher-order modulation formats in coherent receivers are incompatible with the existing NRZ modulation format in deployed PONs. To support a higher-order modulation signal such as QPSK or M-QAM, the transmitter complexity and cost will be higher. Besides, complex DSP in traditional coherent receivers makes cost and power consumption unacceptable for upgrading existing PON components [7].

In recent years, low-complexity quasi/simplified-coherent detection schemes have been proposed to alleviate the bottleneck introduced by traditional coherent and IMDD receivers [7]–[9]. Quasi/simplified coherent detection scheme detects simple intensity modulated signal but uses LO to boost sensitivity of received signal. In contrast to classic coherent link, the receiver's digital signal processing (DSP) can be simplified as phase locking and carrier phase recovery are not required. In addition, there is less need for equalization and chromatic dispersion (CD) compensation, which are essential in APD or SOA-PIN based IMDD links.

This paper proposes an integrated balanced quasi-coherent receiver containing a 2x2 MMI, a pair of balanced PIN

This work is partially funded by FWO, EU POETICS (No 871769) and NEBULA (No 871658). The authors (Joris Lambrecht,previously) are with IDLab, Department of Information Technology, Ghent University - IMEC, 9052 Gent, Belgium.

photodiodes and a high-bandwidth TIA. The received signal power can be optically amplified by beating with an LO, decreasing the impact of the TIA noise. In addition, the RIN caused by the LO laser is largely suppressed by employing balanced photodiodes [10], [11] in the proposed quasi-coherent configuration. By adjusting the wavelength offset between LO and transmitter laser, the IF can be chosen near 3 dB bandwidth of the receiver front end to suppress the chromatic dispersion induced distortion in the upper sideband. This paper is an extension of our work presented in [12]. Besides the measured results in [12], to fairly compare with the IMDD case, a new assembly including the same integrated PIN germanium photodiode and high-speed TIA was made and measured. Furthermore, we investigate the chromatic dispersion tolerance and its relationship with various IF choices at different data rates for the quasi-coherent receiver. For 10.1 dBm LO power, measurements show that the OMA sensitivity at the BER reference level 1e-2 of the proposed quasi-coherent receiver is -25.8 dBm (average received optical power is -27 dBm) for B2B and -19.8 dBm after transmission in 5 km SSMF in C-band at 1550nm. This constitutes a 13 dB improvement in B2B and >16 dB enhancement after 5 km SSMF transmission at 1550nm over the IMDD scheme for 50 Gb/s NRZ. At 50Gb/s NRZ, the power penalty due to chromatic dispersion after 5 km SSMF transmission at 1550nm is more than 4 dB lower than the IMDD scheme at a BER of 1e-2. The G.657 SSMF [13] is used in experiment whose chromatic dispersion value is 17ps/(nm*km) (typical case) at 1550 nm. 5km transmission in SSMF at 1550 nm accumulates total chromatic dispersion of 85ps/nm. By reducing the LO power for high input signal powers, a dynamic range exceeding 24 dB can be covered for the BER reference level 1e-2, which satisfies class C+ level in ITU-T 50G PON PMD layer specification[1]. Furthermore, for 40 Gb/s NRZ, the measured OMA sensitivity at a BER of 1e-2 is -27.8 dBm and -21.8 dBm for B2B and 10 km SSMF at 1550 nm respectively. The proposed balanced quasi-coherent receiver front end significantly improves the chromatic dispersion tolerance compared to the IMDD scheme for 40 Gb/s NRZ in a 10 km SSMF transmission at 1550 nm. To verify the tolerance to IF variation due to wavelength drift in a practical laser implementation in the B2B case, the BER curves under different IF from 34 GHz to 40 GHz have been measured for 40Gb/s NRZ. We find that sensitivity deviation at BER 1e-2 is negligible for practical implementations. Finally, we show the choice of IF for the best chromatic dispersion tolerance for different data rates within a certain length of SSMF. All of these results for the proposed quasi-coherent RX front end are achieved without any complex DSP such as equalization, chromatic dispersion compensation and phase locking.

II. The Principle of Proposed Scheme

Fig. 1(a) shows the simplified block diagram of the proposed balanced quasi-coherent integrated receiver front end. Signal and LO are coupled into the photonic IC (PIC) via a grating coupler (GC) with 3 dB insertion loss at 1550 nm and mixed through a 2x2 MMI. Then, the two outputs from the MMI are fed separately into two on-chip photodiodes. Based on the 180 degree hybrid principle of 2x2 MMI, common-mode components are eliminated after the squaring and subtraction operation in the balanced photodiodes, and the differential components are added constructively. Equations (1)-(2) represent the currents flowing through the balanced PDs ($i_{pd,1}$ and $i_{pd,2}$ in Fig.1(a)). The differential current flowing into the TIA in Eq. (3) is got after balanced PDs ($i_{pd,diff}$ in Fig.1 (a)). R is the photodiode responsivity, P_{LO} and P_S is the power of LO and received signal before GC respectively, f_0 is intermediate frequency.

$$i_{pd,1} = \frac{1}{2}RP_{LO} + \frac{1}{2}RP_S + R\sqrt{P_{LO}P_S}\cos(2\pi f_0 t + \varphi) \tag{1}$$

$$i_{pd,2} = \frac{1}{2}RP_{LO} + \frac{1}{2}RP_S - R\sqrt{P_{LO}P_S}\cos(2\pi f_0 t + \varphi) \tag{2}$$

$$i_{pd,diff} = 2R\sqrt{P_{LO}P_S}\cos(2\pi f_0 t + \varphi) \tag{3}$$

$$i_{pd,IMDD} = RP_S \tag{4}$$

$$K = i_{pd,diff}/i_{pd,IMDD} = 2\sqrt{P_{LO}/P_S} \tag{5}$$

The AC signal components are amplified significantly thanks to a strong LO. Dividing amplitude of Eq. (3) by PD current value in direct detection as shown in Eq. (4), we got K in Eq. (5) representing AC signal gain compared with direct detection case after using LO to boost signal power, depending on ratio of LO power to input signal power. The RIN introduced by the LO is suppressed thanks to the balanced operation [10], [11]. For the balanced receiver to operate optimally, it is important that each photodiode generates equal amounts of DC current. Due to manufacturing tolerances, the MMI will deviate slightly from the ideal splitting ratio, and the photodiode responsivity can differ slightly. To tune the splitting ratio, two waveguide heaters are placed next to the MMI. By applying a thermal gradient across the MMI, the optical power can be steered slightly. This allows us to reduce unwanted DC current flowing into the TIA and improves the common-mode rejection. Therefore, there is no need for dedicated DC block capacitors in front of the TIA: a DC-coupled receiver architecture can be beneficial, particularly for burst-mode signal detection in PON's upstream [14].

Fig. 2 shows how the proposed detection scheme operates in the frequency domain. A baseband signal (e.g. NRZ with data rate R_b) modulated by an optical carrier at a certain wavelength λ is mixed with LO within a wavelength offset $\Delta\lambda$ after 2x2 MMI and PDs. The optical signal is downconverted to an intermediate frequency signal carrying the NRZ signal with a center frequency f_0. A linear TIA will further amplify the IF signal. Due to bandwidth limitations from BPD and bonding wire inductance, the upper sideband of IF signal will be partially filtered, as shown in Eq.(6) and Fig.2. After squaring, half of the IF signal power will be moved to the baseband and the NRZ signal can be recovered. The other half of the IF signal power will be moved around $2f_0$ and removed by a low pass filter as shown in Eq.(7) and Fig.(2). Depending

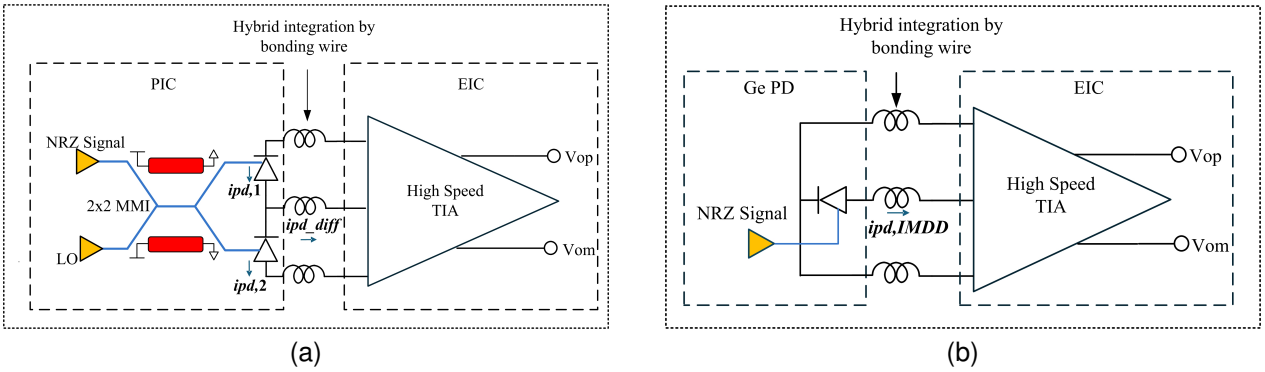

Fig. 1. Different optical Rx front ends. (a) Proposed quasi-coherent Rx front end (b) IMDD RX front end.

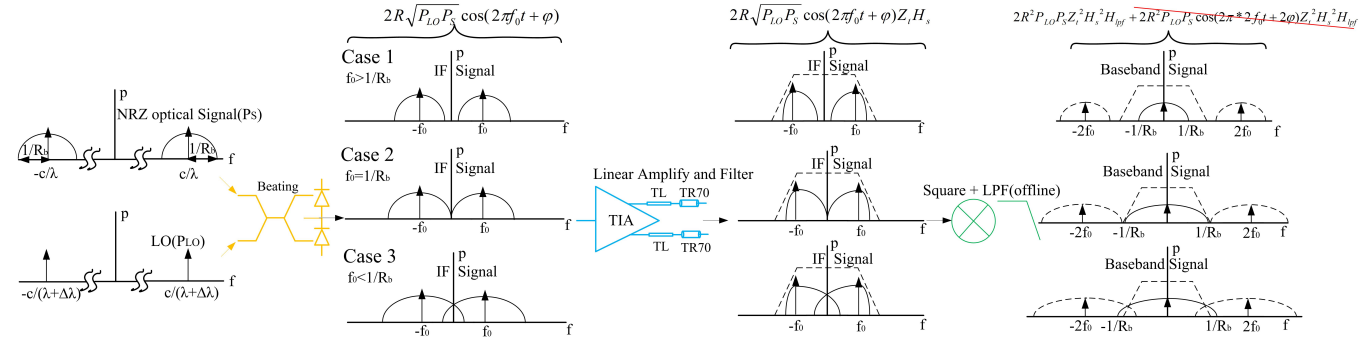

Fig. 2. Signal detection in frequency domain.

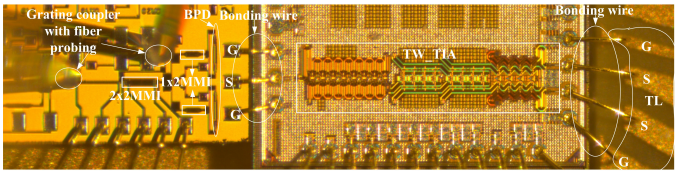

Fig. 3. Hybrid integration of PIC and EIC.

on the value of R_b and f_0, there are three different cases shown in Fig.2. If only the IF signal is considered without any noise, we can get a clean and complete baseband signal in both case 1 and case 2. In case 3, the baseband signal experiences some distortion due to the overlap of the double IF signal and baseband signal. The center frequency of the IF can be chosen near the 3dB BW of the TIA, where the upper sideband is largely filtered and the chromatic dispersion induced distortion in the upper sideband is suppressed. The demodulation after the TIA can be realized either by using an analog envelope detector [15] or multiplier followed by a low pass filter circuit or by sampling with a high-speed ADC and processing in the digital domain. There is no need for carrier phase locking or recovery at the receiver side. Besides, at the sender side, an IMDD transmitter can be reused instead of a high-order modulation-based coherent transmitter, enabling a more cost-effective and simpler upgrade path for existing TXs in high-bitrate PON systems.

$$TIA_{filtered} = 2R\sqrt{P_{LO}P_S}\cos(2\pi f_0 t + \varphi)Z_t H_s \quad (6)$$

$$Output = 2R^2 P_{LO}P_S Z_t^2 H_s^2 H_{lpf} + 2R^2 P_{LO}P_S \cos(2\pi * 2f_0 t + 2\varphi) Z_t^2 H_s^2 H_{lpf} \quad (7)$$

The integrated quasi-coherent RX front end includes a PIC fabricated in imec's iSiPP50G silicon photonic platform and high-speed integrated TIA fabricated in ST 55nm SiGe BiC-MOS process. The PIC and EIC are integrated via wirebonding on one PCB. Fig. 3 shows the details of the hybrid integrated quasi-coherent front end (including PIC and EIC). Two grating couplers are connected individually to two waveguides which are inputs of a 2x2 MMI. Two heaters are located separately on each side of the 2x2 MMI, controlled by a DC signal. The outputs of the 2x2 MMI are guided to two 1x2 MMIs, after which every two waveguides go into each photodiode, improving the photodiodes' linearity at high optical powers. Each pair of photodiodes is connected in series. The 2x2 MMI has a maximum power imbalance of 0.32 dB. The germanium photodiode has 0.88 A/W responsivity at a 1550 nm wavelength and higher than 45 GHz bandwidth with reverse bias voltage of 2.7V. The high-speed TIA [16] is based on a traveling-wave architecture with measured BW of 62 GHz, highest transimpedance of 76.8 dBohm and input referred integrated noise of 4.75 uArms. (Assuming 64 GHz noise BW, input-referred noise is $18.8\,pA/\sqrt{Hz}$).

In Fig.4 (a) and (b), S-parameter of photodiode(PD) is shown, which is measured by using an RF probe connected to a ME7848A-200 opto-electronic network analyzer. In Fig.4 (c),the blue and black lines are measured electrical frequency

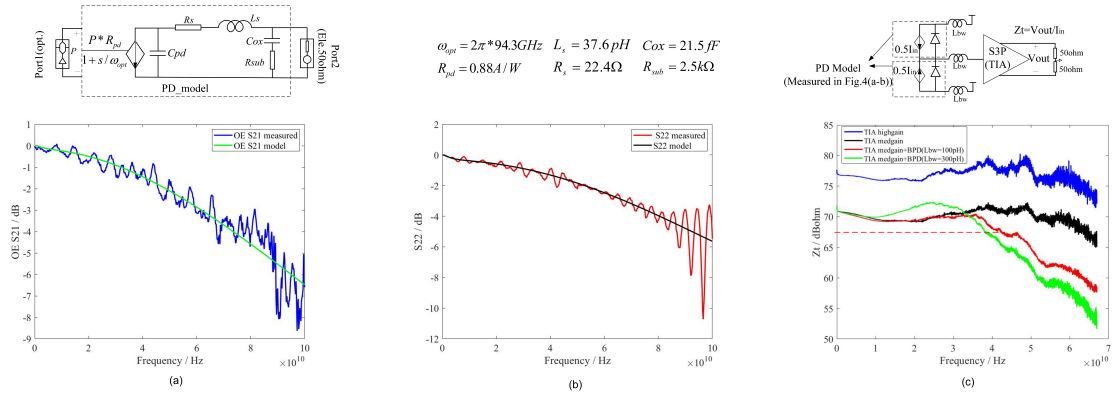

Fig. 4. (a) Measured Optical-Electrical S21 of PD (b) Measured S11 of PD (c) Frequency response of TIA without/within BPD and 100pH/300pH bonding wire

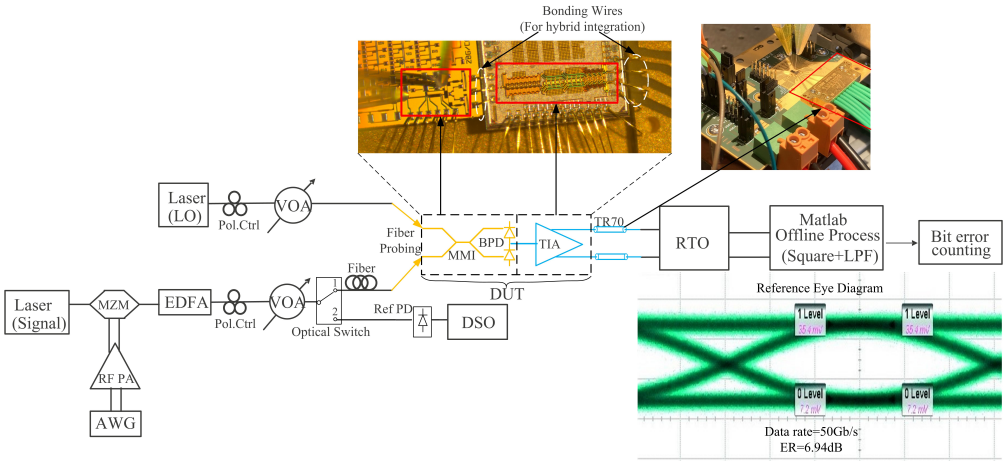

Fig. 5. Experimental Setup and reference eye.

response of TIA at different gain settings without any additional connected loadings at inputs and outputs. During experiment, we set transimpedance of TIA at medium gain to achieve best trade off between gain and linearity. Considering the effect of PIC (especially BW limitation from balanced PDs) and parasitic inductance from bonding wires,co-simulation of measured PD model (in balanced configuration) connected with TIA (measured S-parameter) is also shown in Fig.4(c). The BW of receiver front end is around 40GHz and limited by BPD and parasitic inductance from bonding wire.

III. Experiment Setup

The experiment setup is shown in Fig. 5. An arbitrary waveform generator (Keysight M8196A) with a sample rate of 92 GSa/s is used to generate pseudo random binary sequence (PRBS) data with a length of $2^{15}-1$ at different data rates. After the AWG, a broadband RF amplifier drives a commercial Mach-Zehnder modulator (MZM), biased at its quadrature point. A low linewidth DFB laser (NKT Koheras BASIK) operating in the wavelength range from 1549.45nm to 1550.59 nm is used as a laser source for the transmitter. The value of RIN is smaller than -135dBc/Hz at 10MHz. Following the MZM, the NRZ optical signal is amplified by an Erbium-doped fiber amplifier (EDFA). A programmable variable optical attenuator (VOA) sets the signal power at different values. The same type of low linewidth DFB laser source is used as the LO, whose wavelength is offset to the transmitter laser. The LO power before the grating coupler is 10.1 dBm. Finally, the PIC is fiber probed using two cleaved fibers. Different lengths of SSMF with typical CD vaule of 17ps/(nm*km) at 1550 nm are inserted into the channel to evaluate the impact of chromatic dispersion on the receiver. Since the grating couplers are polarization sensitive, two polarization controllers are added to optimize the coupling efficiency. An optical switch in the signal path determines whether the signal flows into the fiber link or a reference photodiode (XPDV3120R). The reference photodiode connected to a digital sampling oscilloscope (DSO) is used to check the eye quality of the transmitted signal. The TIA outputs are wirebonded to the RF PCB and connected to a real-time oscilloscope (RTO) using an Ardent TR70 coaxial connector. Demodulation of the received NRZ signal has been performed offline in Matlab, including a simple square function and a 5th-order Butterworth low pass filter with a cutoff frequency set to 70% of the bit rate.An envelope detector [15] can also realize these operations in the analog domain. No extra equalization or chromatic dispersion compensation was used. The BER is calculated using the bit error counting method. For the comparison experiment in the

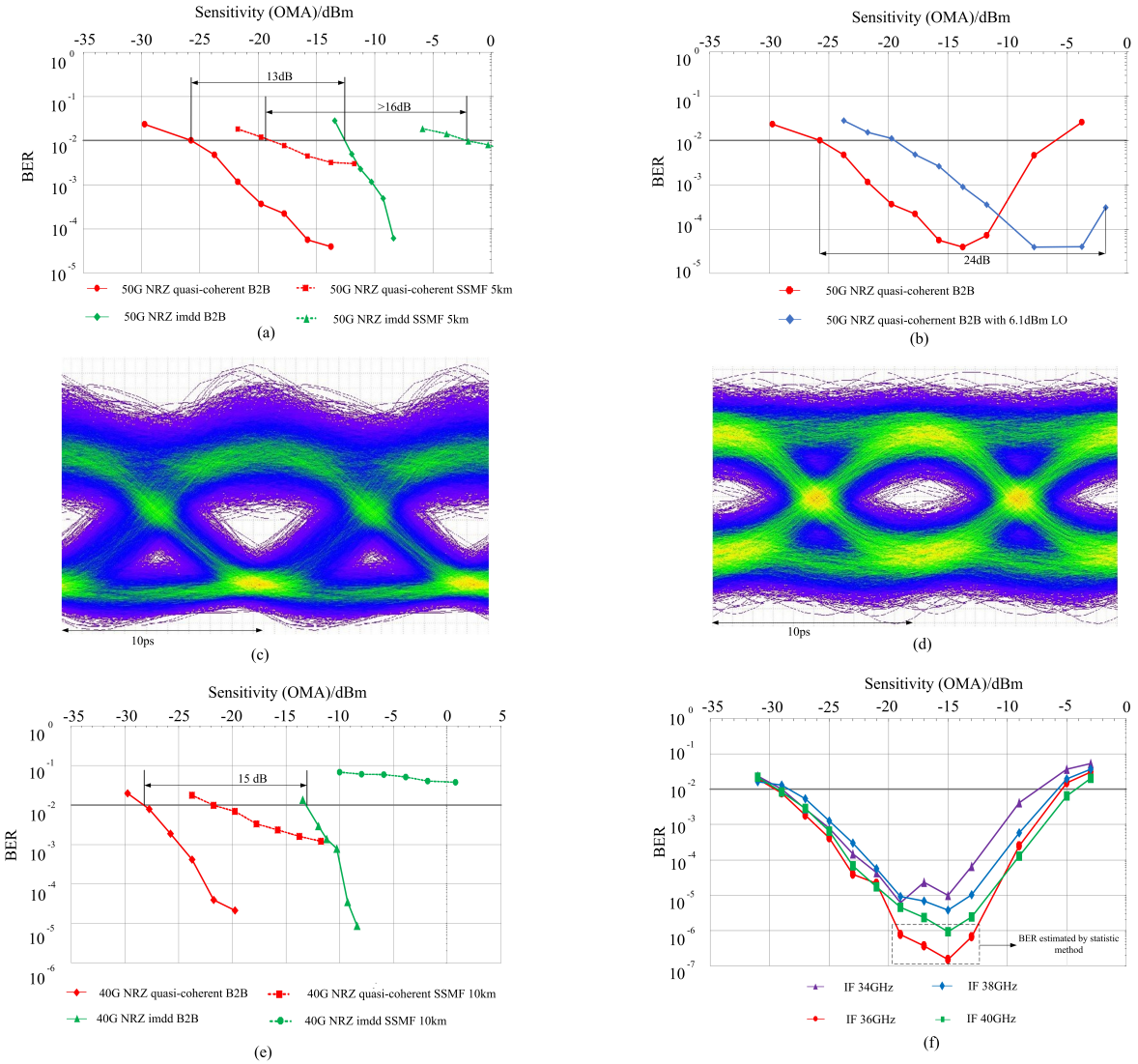

Fig. 6. (a) Comparison between QC RX and IMDD RX for 50Gb/s NRZ (b) Dynamic range in QC RX for 50Gb/s NRZ (c) Output eye diagram from QC RX for B2B 50Gb/s NRZ (d) Output eye diagram from IMDD RX for B2B 50Gb/s NRZ(e) Comparison between QC RX and IMDD RX for 40Gb/s NRZ (f) BER curve for 40Gb/s NRZ with different f_0 of IF

IMDD case, the DUT in Fig.5 is replaced with the same integrated germanium photodiode wire-bonded with TIA in the way shown in Fig. 1(b), and the path from LO to DUT is disconnected.

IV. Experiment Results and Discussion

The 50G NRZ eye diagram from reference PD is shown in Fig.5 with 0 dBm received optical power and 6.94 dB extinction ratio. All the measurements, both for the proposed scheme as well as the IMDD scheme, are based on the same integrated germanium photodiode and TIA. Fig.6 (a) is the BER curve for 50 Gb/s NRZ, including the quasi-coherent Rx and the IMDD RX. The sensitivity value is calculated based on the OMA of the received optical signal power before the grating coupler, as the grating coupler is also regarded as part of the receiver front end in practical implementations. In the B2B case, for the quasi-coherent RX, sensitivity in OMA at reference BER level 1e-2 is -25.8 dBm, which is 13 dB better than IM-DD RX. After 5 km SSMF transmission in at 1550nm, quasi-coherent RX realizes -19.8 dBm sensitivity in OMA at BER 1e-2, which yields more than 16 dB improvement over the IMDD RX. The type of fiber used in measurement is single mode ITU-T G.657. The CD value for single mode fiber G.657 is 17 ps/(nm*km) in C-band (at 1550 nm in typical case) and 3.7 ps/(nm*km) in O-band (at 1342nm in worst case) [13]. Considering chromatic dispersion value only, 5km transmission at 1550nm is equivalent to 23 km at 1342nm of SSMF. [17] demonstrates 5km SSMF transmssion at 1550nm can be equivalent to 20km SSMF transmission at 1342nm. Measurement results and [17] both suggest that the proposed quasi-coherent receiver could support 20km fiber reach in new 50G PON standard at 1342nm in O-band, which meets the fiber reach specification in ITU-T G.9804 for 50G PON [1]. Fig.6(c) and (d) respectively show the eye diagram for quasi-coherent RX and IMDD RX at the best BER value in Fig.5 (b). Due to center frequency f_0 of IF signal is 40GHz, which is

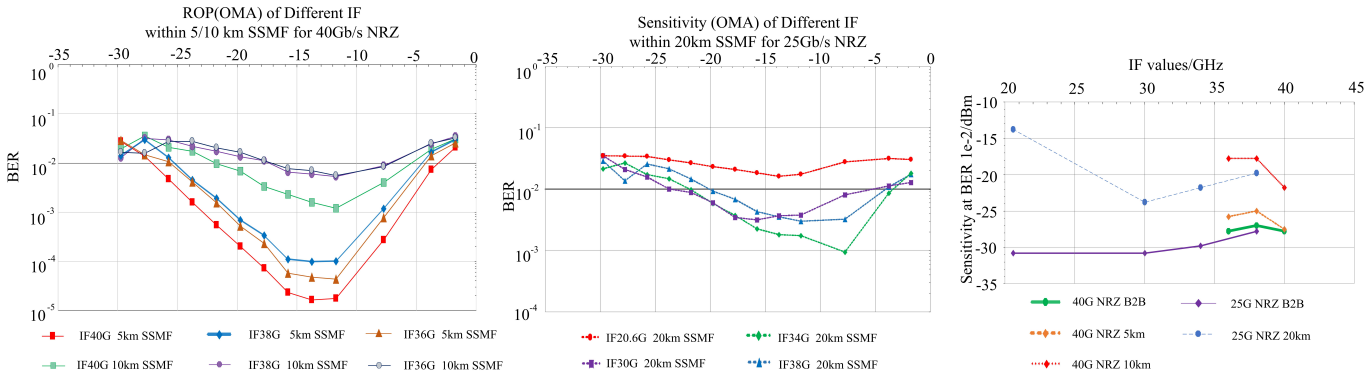

Fig. 7. Relationship between IF value and CD tolerance. (a) CD tolerance at 40G case (b) CD tolerance at 25G case. (c)Sensitivity dependence on IF values

smaller than data rate R_b (50Gb/s) . After square opearation, spectrum contamination exists as shown in Fig.2. Thus, the eye diagram for quasi-coherent RX is distorted. The LO power can be tuned 4 dB lower to cover a >24 dB dynamic range, which satisfies the class C+ level in the ITU-T 50G PON PMD layer specification. In a practical implementation, the LO power can be tuned using an embedded feedback loop. Furthermore, Fig. 6(e) shows the sensitivity results for 40 Gb/s NRZ in both the B2B case and 10 km SSMF case. The sensitivity in OMA at a BER of 1e-2 for the quasi-coherent RX is -27.8 dBm. Compared with the IMDD RX in the B2B cases at the same BER level, the quasi-coherent Rx achieves about 15 dB of sensitivity enhancement. After 10 km SSMF transmission in C-band, the quasi-coherent RX displays a better chromatic dispersion tolerance than the IMDD RX. At a BER of 1e-2, the quasi-coherent RX only has a 5.8dB power penalty while the sensitivity for IMDD RX degrades significantly after 10 km transmission in SSMF at 1550 nm. The improved chromatic dispersion tolerance of the quasi-coherent RX mainly stems from filtering most parts of the upper sideband of the downconverted IF signal by the proper choice of intermediate frequency value. Although filtering the upper sideband loses some useful signal power, chromatic dispersion induced distortion is removed, and LO gain can compensate for the loss induced by filtering. To create Fig.6(a) and (e), a 40 GHz IF is chosen for both 50 Gb/s NRZ and 40 Gb/s NRZ cases by tuning the wavelength offset between LO and transmit laser. IF variations due to wavelength drifting in 8 hours during the measurement are smaller than 1 GHz. To verify the tolerance of the quasi-coherent front end to variations in IF, we measured B2B case BER for 40 Gb/s NRZ at different IFs ranging from 34 GHz to 40 GHz, which is plotted in Fig. 6(f). There are small sensitivity variations among different IF cases. However, for the BER case of 1e-2 , the sensitivity deviations due to different IFs can be ignored. In Fig. 6(f), the BER values smaller than 1e-6 are estimated by a statistic method because the captured data from the RTO is only 10 μs long. The minimal measurable BER is 2.5e-6 for a 10 μs waveform(1 error over 400000 symbols at 40G baud rate). Figure 7 shows the relationship between IF and CD tolerance for 40G and 25G NRZ. At 40Gb/s NRZ in Fig.7(a), moving the IF from 36GHz to 40GHz, the CD tolerance becomes better in both 5km and 10km SSMF cases. At 25Gb/s in Fig.6(b), moving the IF from 20.6GHz to 30GHz, there is a significant improvement in CD tolerance for 20km of SSMF. Moving the IF to values larger than 30GHz will induce a slight sensitivity degradation. In Fig.6(c), we show the sensitivity dependence on the IF for different data rates using various lengths of SSMF at a BER of 1e-2. There is a trade-off when choosing the IF to get the best sensitivity for transmission at different data rates and lengths of fiber. The IF can be set to a higher value (but still around 3dB BW of the whole receiver), and the upper sideband is filtered more thoroughly. In the 40Gb/s case, the sensitivity improves by filtering more of the upper sideband, making up for the signal power loss. For 25Gb/s case, moving the IF beyond 30GHz only yields marginal BER improvements from filtering the upper sideband. A comparison with the state of the art is shown in Table I. Compared with IMDD implementation using an APD in work [2] at 50 Gb/s NRZ, we achieve 5.6 dB improvement of sensitivity without any equalization in DSP. Compared with the IMDD implementation using an SOA for optical signal boosting in work [5] at 50 Gb/s NRZ, there is 2.4 dB enhancement while SOA-UTC-PD has about 60 A/W responsivity with 18.1 dBm (65 mW) power consumption. Compared to a similar quasi-coherent scheme [8] having a 4.9 dB higher LO power, the average received optical power in our proposed balanced quasi-coherent RX is 6 dB better at 25 Gb/s NRZ on BER 1e-2. At 50 Gb/s NRZ, compared to EDB detection with SOA+PIN-TIA in [4], an average sensitivity enhancement of 3 dB is achieved at BER threshold 1e-3. At 25 Gb/s NRZ, there is 7.2 dB improvement compared to EDB detection with the APD in [4] of BER 1e-3. Since the photonic integrated circuit is polarization dependent, we used polarization controllers in the experimental setup to align the polarization of the signal and LO. For practical PON implementation, 2D grating couplers or edge-couplers with polarization splitter-rotator (PSR) can be implemented to minimize polarization dependence [18], [19].

TABLE I
COMPARISON WITH STATE-OF-THE-ART

	This work	[2]JLT'23	[5]OFC'24	[4] JLT'16	[8] JLT'20	[7]JLT'18
Detection method	Balanced quasi-coherent 2x2 MMI	IMDD APD	IMDD SOA+PIN	IMDD APD /SOA+PIN	Quasi-coherent 2x2 MMI	Simplified coherent 3x3 fiber coupler
OMA Sensitivity at BER 1e-2 for 50G NRZ /dBm	-25.8* -19.8**	-18.2* -23.7*!	-23.4* -24.3*!	N.A.	N.A.	N.A.
Average Sensitivity at BER 1e-3 for 50G NRZ /dBm	-23*	-16*	-22.3*	-20*	N.A.	N.A.
Average Sensitivity for 25G NRZ /dBm	-31*(1e-2) -29.6*(1e-3)	N.A.	N.A.	-22.4*(1e-3)	-25*(1e-2) -22.3*(1e-3)	-37*(1e-2) -35*(1e-3)
LO or SOA Power/dBm	10.1	no	18.1	N.A.	15	12
Dynamic range at BER 1e-2/dB	24(50G)	21.7(50G)	20(50G)	18(25G)	N.A.	N.A.
Photodiode type	PIN	APD	PIN(integrated with SOA)	APD/PIN	PIN	PIN
Wavelength Range	C-band	O-band	O-band	O-band	C-band	C-band

*B2B without equalization **5km SSMF without equalization !With 13 taps FFE and 1 tap DFE

V. CONCLUSION

An integrated balanced quasi-coherent RX front end is proposed and measured. At a BER level of 1e-2 for 50 Gb/s NRZ, corresponding to pre-FEC limit in ITU-T G.9804, -25.8 dBm OMA sensitivity is achieved in B2B case, and -19.8 dBm OMA sensitivity is realized after 5 km SSMF transmission in C-band at 1550nm. Measurement results show that total chromatic dispersion of 85 ps/nm can be handled for BER value lower than 1e-2. A dynamic range exceeding 24 dB is realized, which meets the class C+ level in ITU-T 50G PON PMD layer specification assuming 8.5 dBm transmitter launch power [1]. These results are achieved without any complex DSP such as equalization, CD compensation and phase locking/recovery.

ACKNOWLEDGMENTS

This work is partially funded by FWO, EU POETICS (No 871769) and NEBULA (No 871658).

REFERENCES

[1] ITU-T, *50-Gigabit-capable passive optical networks(50GPON):PMD layer specification*. ITU-T G.9804.3(2021)Amd.1, 02/2023.

[2] G. Coudyzer, M. Verplaetse, B. Van Lombergen, R. Borkowski, T. Gurne, M. Straub, Y. Lefevre, P. Ossieur, R. Bonk, W. Coomans, J. Maes, and X. Yin, "100 Gbit/s PAM-4 Linear Burst-Mode Transimpedance Amplifier for Upstream Flexible Passive Optical Networks," *Journal of Lightwave Technology*, vol. 41, no. 12, pp. 3652–3659, 2023.

[3] J. C. Campbell, "Recent Advances in Telecommunications Avalanche Photodiodes," *Journal of Lightwave Technology*, vol. 25, no. 1, pp. 109–121, Jan 2007.

[4] X. Yin, J. Van Kerrebrouck, J. Verbist, B. Moeneclaey, X.-Z. Qiu, J. Bauwelinck, D. Lanteri, F. Blache, M. Achouche, and P. Demeester, "An Asymmetric High Serial Rate TDM-PON With Single Carrier 25 Gb/s Upstream and 50 Gb/s Downstream," *Journal of Lightwave Technology*, vol. 34, no. 2, pp. 819–825, 2016.

[5] L. Breyne, C. Caillaud, T. Gurne, J.-F. Paret, M. Straub, G. Coudyzer, K. Mekhazni, and M. Verplaetse, "50G Burst-Mode Receiver Using Monolithic SOA-UTC and Burst-Mode TIA," in *2024 Optical Fiber Communications Conference and Exhibition (OFC)*, 2024, pp. 1–3.

[6] T. A. Eriksson, T. Almeida, H. Åhlfeldt, M. S. Erkılınç, X. Chen, J. Hellman, A. Kumpera, A. Rashidinejad, A. Napoli, C. R. S. Fludger, P. Lembre, J. Bäck, M. Olson, and D. Welch, "Real-time bidirectional coherent point-to-multipoint passive optical network," in *49th European Conference on Optical Communications (ECOC 2023)*, vol. 2023, 2023, pp. 487–490.

[7] V. Houtsma and D. van Veen, "Bi-Directional 25G/50G TDM-PON With Extended Power Budget Using 25G APD and Coherent Detection," *Journal of Lightwave Technology*, vol. 36, no. 1, pp. 122–127, 2018.

[8] J. A. Altabas, O. Gallardo, G. S. Valdecasa, M. Squartecchia, T. K. Johansen, and J. B. Jensen, "DSP-Free Real-Time 25 GBPS Quasicoherent Receiver With Electrical SSB Filtering for C-Band Links up to 40 km SSMF," *Journal of Lightwave Technology*, vol. 38, no. 7, pp. 1785–1788, 2020.

[9] M. G. Saber, M. Osman, D. Patel, A. Samani, E. El-Fiky, M. S. Alam, K. A. Shahriar, Z. Xing, M. Jacques, B. Dortschy, G. Vall-Llosera, P. J. Urban, F. Cavaliere, S. Lessard, and D. V. Plant, "Demonstration of a 120° hybrid based simplified coherent receiver on SOI for high speed PON applications," *Opt. Express*, vol. 26, no. 24, pp. 31 222–31 232, Nov 2018.

[10] C. Bruynsteen, M. Vanhoecke, J. Bauwelinck, and X. Yin, "Integrated balanced homodyne photonic–electronic detector for beyond 20GHz shot-noise-limited measurements," *Optica*, vol. 8, no. 9, pp. 1146–1152, Sep 2021.

[11] B. Zhang, C. Malouin, and T. J. Schmidt, "Design of coherent receiver optical front end for unamplified applications," *Opt. Express*, vol. 20, no. 3, pp. 3225–3234, Jan 2012.

[12] C. Wang, C. Bruynsteen, J. Declercq, J. Lambrecht, B. Moeneclaey, N. Singh, and X. Yin, "Low-complexity balanced quasi-coherent receiver with integrated 2×2 mmi balanced photodiode and TIA for 50G PON," in *49th European Conference on Optical Communications (ECOC 2023)*, vol. 2023, 2023, pp. 1107–1110.

[13] ITU-T, *Characteristics of a bending-loss insensitive single-mode optical fibre and cable G.657*. ITU-T, 02/2023.

[14] X.-Z. Qiu, X. Yin, J. Verbrugghe, B. Moeneclaey, A. Vyncke, C. Van Praet, G. Torfs, J. Bauwelinck, and J. Vandewege, "Fast Synchronization 3R Burst-Mode Receivers for Passive Optical Networks," *Journal of Lightwave Technology*, vol. 32, no. 4, pp. 644–659, 2014.

[15] G. Silva Valdecasa, O. G. Puertas, J. A. Altabas, M. Squartecchia, J. B. Jensen, and T. K. Johansen, "High-Speed SiGe BiCMOS Detector Enabling a 28 Gbps Quasi-Coherent Optical Receiver," *IEEE Transactions on Circuits and Systems II: Express Briefs*, vol. 69, no. 3, pp. 964–968, 2022.

[16] J. Declercq, B. Moeneclaey, J. Lambrecht, C. Bruynsteen, N. Singh, S. Niu, P. Ossieur, and X. Yin, "A 100 GBd PAM-4 optical receiver using a SiGe BiCMOS traveling-wave EIC and a silicon photonic Ge photodetector," in *49th European Conference on Optical Communications (ECOC 2023)*, 2023, pp. 1378–1381.

[17] M. Tao, J. Zheng, X. Dong, K. Zhang, L. Zhou, H. Zeng, Y. Luo, S. Li, and X. Liu, "Improved Dispersion Tolerance for 50G-PON Downstream Transmission via Receiver-Side Equalization," in *2019 Optical Fiber Communications Conference and Exhibition (OFC)*, 2019, pp. 1–3.

[18] H. Xu and Y. Shi, "Ultra-broadband silicon polarization splitter-rotator based on the multi-mode waveguide," *Opt. Express*, vol. 25, no. 15, pp. 18 485–18 491, Jul 2017.

[19] P. Dong, X. Liu, S. Chandrasekhar, L. L. Buhl, R. Aroca, and Y.-K. Chen, "Monolithic Silicon Photonic Integrated Circuits for Compact 100 $^{+}$Gb/s Coherent Optical Receivers and Transmitters," *IEEE Journal of Selected Topics in Quantum Electronics*, vol. 20, no. 4, pp. 150–157, 2014.